

# Hyperphosphorylation and Aggregation of Tau in Laforin-deficient Mice, an Animal Model for Lafora Disease\*<sup>§</sup>

Received for publication, April 17, 2009, and in revised form, June 13, 2009. Published, JBC Papers in Press, June 19, 2009, DOI 10.1074/jbc.M109.009688

Rajat Puri<sup>‡</sup>, Toshimitsu Suzuki<sup>§</sup>, Kazuhiro Yamakawa<sup>§</sup>, and Subramaniam Ganesh<sup>†1</sup>

From the <sup>‡</sup>Department of Biological Sciences and Bioengineering, Indian Institute of Technology, Kanpur 208016, India and the <sup>§</sup>Laboratory for Neurogenetics, RIKEN Brain Science Institute, Wako-shi 351-0198, Japan

Lafora progressive myoclonous epilepsy (Lafora disease; LD) is caused by mutations in the *EPM2A* gene encoding a dual specificity protein phosphatase named laforin. Our analyses on the *Epm2a* gene knock-out mice, which developed most of the symptoms of LD, reveal the presence of hyperphosphorylated Tau protein (Ser<sup>396</sup> and Ser<sup>202</sup>) as neurofibrillary tangles (NFTs) in the brain. Intriguingly, NFTs were also observed in the skeletal muscle tissues of the knock-out mice. The hyperphosphorylation of Tau was associated with increased levels of the active form of GSK3 $\beta$ . The observations on Tau protein were replicated in cell lines using laforin overexpression and knockdown approaches. We also show here that laforin and Tau proteins physically interact and that the interaction was limited to the phosphatase domain of laforin. Finally, our *in vitro* and *in vivo* assays demonstrate that laforin dephosphorylates Tau, and therefore laforin is a novel Tau phosphatase. Taken together, our study suggests that laforin is one of the critical regulators of Tau protein, that the NFTs could underlie some of the symptoms seen in LD, and that laforin can contribute to the NFT formation in Alzheimer disease and other tauopathies.

Lafora disease (LD)<sup>2</sup> is an autosomal recessive and a fatal form of progressive myoclonus epilepsy characterized by the presence of Lafora polyglucosan bodies in the affected tissues (1). The symptoms of LD include stimulus-sensitive epilepsy, dementia, ataxia, and rapid neurologic deterioration (1, 2). LD is caused by mutations in the *EPM2A* gene encoding laforin, a dual specificity protein phosphatase, or in the *NHLRC1* gene encoding malin, an E3 ubiquitin ligase (3–7). Both laforin and malin are ubiquitously expressed (3, 5), associated with the endoplasmic reticulum (4, 7), form aggregates upon proteaso-

mal blockade (7), and clear misfolded protein through ubiquitin-proteasome (8). Laforin has two functional domains: a phosphatase domain (dual specificity phosphatase domain; DSPD) and a carbohydrate binding domain (CBD) (9). The CBD helps laforin to target to the glycogen particle and to the Lafora bodies (9, 10), and the DSPD of laforin dephosphorylates carbohydrate moieties (11). Recent studies have further shown that laforin and malin together regulate the cellular levels of PTG, the adaptor protein targeting to glycogen, and that the loss of either malin or laforin results in increased levels of PTG that eventually lead to excessive glycogen deposition (12–14). Although this model explains the genesis of Lafora bodies, the molecular etiology of LD is yet to be understood. For example, unlike this cell line study (12), the presence of Lafora bodies does not lead to neuronal cell death in the two murine models of LD (10, 15), and no difference in the level of PTG was seen in laforin-deficient mice (16).<sup>3</sup> However, widespread degeneration of neurons was seen in laforin-deficient mouse with the absence of Lafora bodies, suggesting that the polyglucosan bodies may not play a primary role in the epileptogenesis (15). The laforin dominant-negative transgenic mice line also developed Lafora bodies but had no signs of neurodegeneration or epileptic seizures (10). Thus, the neurodegenerative changes are likely to underlie the etiology of some of the LD symptoms (1). The mouse model developed by the knockdown of the *Epm2a* gene exhibited a majority of the symptoms known in LD, including the ataxia, spontaneous myoclonic seizures, EEG epileptiform activity, and impaired behavioral responses (15). The knock-out animals showed a number of degenerative changes that include swelling and/or loss of morphological features of mitochondria, endoplasmic reticulum, Golgi apparatus, and the neuronal processes (15). Preliminary histochemical investigations have also suggested the possible presence of neurofibrillary tangles (NFTs) in the knock-out mice (17). In this study, we have characterized the biochemical properties of Tau protein in the animal model of LD and identified laforin as an interacting partner of Tau. Our study identifies laforin to be one of the critical regulators of Tau protein and suggests that the Tau pathology might underlie some of the symptoms seen in LD.

## EXPERIMENTAL PROCEDURES

**Mice and Tissue Harvesting**—The characterization of laforin-deficient mice has been described previously (15). The animals were maintained at the RIKEN Brain Science Institute animal facilities according to the Institute guidelines for the

\* This work was supported in part by sponsored research grants from the Life Science Research Board and the Department of Science & Technology (to S. G.), the Japan Society of the Promotion of Science and the RIKEN Brain Science Institute (to K. Y.), and a Council of Scientific and Industrial Research student fellowship and a Company of Biologists traveling fellowship (to R. P.).

<sup>§</sup> The on-line version of this article (available at <http://www.jbc.org>) contains supplemental Figs. S1 and S2.

<sup>1</sup> To whom correspondence should be addressed: Dept. of Biological Sciences and Bioengineering, Indian Institute of Technology, Kanpur-208016, India. Tel.: 91-512-259-4040; Fax: 91-512-259-4010; E-mail: sganesh@iitk.ac.in.

<sup>2</sup> The abbreviations used are: LD, Lafora disease; DSPD, dual specificity phosphatase domain; CBD, carbohydrate binding domain; PTG, protein targeting to glycogen; NFT, neurofibrillary tangle; E3, ubiquitin-protein isopeptide ligase; PKA, protein kinase A; AKT, protein kinase B; PP2A, protein phosphatase 2A; CDK5, cyclin-dependent kinase 5; GFP, green fluorescent protein.

<sup>3</sup> R. Puri, T. Suzuki, K. Yamakawa, and S. Ganesh, unpublished observations.

## Hyperphosphorylation of Tau in Laforin-deficient Mice

treatment of experimental animals. Animals of 4-, 6-, or 10-month-old age groups were sacrificed by cervical dislocation, and selected tissues were dissected and fixed in appropriate fixatives or quickly frozen in liquid nitrogen and stored at  $-80^{\circ}\text{C}$  until further analysis.

**Tissue Extraction and Subcellular Fractionation**—Brain and muscle tissues were homogenized in Tris-buffered saline containing protease and phosphatase inhibitors and used for immunoblotting analysis. The Sarkosyl-soluble and -insoluble fractions of NFTs were extracted as described (18).

**Antibodies**—The following monoclonal antibodies, obtained as gifts from Dr. Peter Davies, were used for detecting the Tau protein: CP13 for phospho-Ser<sup>202</sup> Tau, PHF1 for phospho-Ser<sup>396</sup> Tau, and TGF5 for all forms of Tau. In addition, antibodies from Innogenetics (antibody AT8) and GenScript for the detection of phospho-Ser<sup>202</sup> and an antibody from Epitomics (antibody E178) for the detection of phospho-Ser<sup>396</sup> were also used. Antibodies for Gsk3 $\beta$ , phospho-Ser<sup>9</sup> Gsk3 $\beta$ , protein kinase B (AKT), and Ser<sup>473</sup> phospho-AKT were purchased from Cell Signaling Technology. Antibodies for protein phosphatase 2A (PP2A), Tyr<sup>307</sup> phospho-PP2A, cyclin-dependent kinase 5 (CDK5), Ser<sup>159</sup> phospho-CDK5, protein kinase A (PKA), Ser<sup>96</sup> phospho-PKA, and PP1 were purchased from Santa Cruz Biotechnology, Inc. (Santa Cruz, CA). Anti-GFP and anti-Myc tag antibodies were purchased from Roche Applied Science, and anti- $\gamma$ -tubulin, anti-FLAG, and anti-V5 antibodies were from Sigma. Anti-ubiquitin antibody was purchased from Dako, and the secondary antibodies were obtained from Jackson ImmunoResearch. Anti-laforin antibody was raised in rabbits using a synthetic peptide corresponding to amino acid residues 85–100 of the murine laforin sequence.

**Immunohistochemical and Histopathological Analyses**—Immunohistochemical analysis was done on formalin-fixed, paraffin-embedded sections and was reacted with appropriate antibody, as described previously (8, 15). They were visualized for light microscopy using diaminobenzidine-conjugated avidin-biotin complex kit (Vectastain ABC Elite; Vector Laboratories). For immunofluorescence staining, sections were processed with appropriate secondary antibodies that were conjugated with rhodamine or fluorescein isothiocyanate and visualized using an epifluorescence microscope, as described (8, 15). Bielschowsky's silver staining was done on paraffin embedded brains sections as described previously (19).

**Ultrastructural Analysis**—For electron microscopy studies, the Sarkosyl-insoluble materials, isolated from the laforin-deficient mice, were mildly sonicated and dispersed in phosphate-buffered saline. For negative staining, the samples were first absorbed onto glow-discharged supporting membranes on 300-mesh grids and then treated with 2% uranyl acetate, dried, and observed with a FEI Technai 20 U Twin electron microscope. For immunogold labeling, the samples were prefixed by floating the grids on drops of 4% paraformaldehyde in 0.1 M phosphate buffer for 5 min. After washing, the grids were incubated with primary antibody followed by 10-nm colloidal gold-conjugated secondary antibody and processed for negative staining with 2% sodium phosphotungstic acid and observed as described (20).

**Expression Constructs**—The expression vectors containing Myc- or GFP-tagged wild-type or mutant forms of laforin were described previously (7, 8). Expression constructs for the FLAG-tagged laforin were generated by cloning the coding regions of the *EPM2A* gene into the pcDNA expression vector (Invitrogen). The short hairpin RNA knockdown constructs for the *Epm2a* gene were purchased from Open Biosystems and validated in one of our recent studies (8). The expression constructs for V5-tagged Tau and its mutant form were generously provided by Dr. Michael Hutton.

**Cell Culture, Transfection, and Pull-down Assays**—COS-7 or Neuro2A cells were grown in Dulbecco's modified Eagle's medium (Sigma) supplemented with 10% (v/v) fetal calf serum, 100 units/ml penicillin, and 100  $\mu\text{g}/\text{ml}$  streptomycin. All cells were grown at  $37^{\circ}\text{C}$  in 5%  $\text{CO}_2$ . Transfections were performed using Lipofectamine 2000 transfection reagent (Invitrogen) according to the manufacturer's protocol. Neuro2A cells were differentiated into neurons by culturing them in 1% fetal bovine serum as described (21). To establish the physical interaction between laforin and Tau proteins, we used the expression construct that code for polyhistidine-tagged Tau (22). Lysates of cells that had expressed His-tagged Tau with desired protein were incubated with  $\text{Ni}^{2+}$ -affinity resin (Sigma) for 2 h at  $4^{\circ}\text{C}$  and processed for pull-down assays as recommended by the manufacturer. Pulled down products were detected by immunoblotting using specific antibodies.

**In Vitro Dephosphorylation Assay**—The histidine-tagged Tau protein, transiently overexpressed in COS-7 cells, was hyperphosphorylated by treating the cells with wortmannin and affinity-purified using nickel resins. Similarly, the His-tagged laforin or its mutant Q293L was expressed and purified as described (23). The nickel resin-bound Tau was mixed with wild-type laforin or its mutant in the phosphatase assay buffer (50 mM HEPES, pH 6, 50 mM NaCl, 5 mM EDTA, 50 mM  $\beta$ -mercaptoethanol) and incubated for 2 h at  $37^{\circ}\text{C}$ . A control reaction was performed in parallel, wherein the Tau protein was incubated with nickel resins treated with cell lysates that did not express His-tagged laforin. The reaction products were finally mixed with SDS sample buffer, boiled, and analyzed by immunoblotting.

**Immunoprecipitation**—Tissue or cell lysates were preincubated with protein G-Sepharose (Bangalore Genei, India) for 2 h at  $4^{\circ}\text{C}$  and then incubated with anti-laforin or anti-GSK3 $\beta$  antibody (as indicated) for 1 h at  $4^{\circ}\text{C}$ . After incubation, protein G-Sepharose was used for precipitation. The beads were washed with lysis buffer four times and then eluted with SDS sample buffer for immunoblot analysis as described (24).

**GSK3 $\beta$  Activity Assay**—GSK3 $\beta$  activity was measured as described previously (25) after immunoprecipitation of GSK3 $\beta$  from 100  $\mu\text{g}$  of protein. Immobilized immune complexes were washed twice with lysis buffer and twice with kinase reaction buffer and incubated with phosphoglycogen synthase peptide-2 substrate (Upstate Biotechnology) and [ $\gamma$ -<sup>32</sup>P]ATP for 30 min at  $30^{\circ}\text{C}$ . After this incubation, an aliquot of samples was placed on phosphocellulose disc (Whatman 31ET CHR filter paper), air-dried, and washed three times in 0.75% phosphoric acid and once with acetone. Radioactivity in the phosphocellulose disc was counted in a  $\beta$ -counter (PerkinElmer Life Sciences).

**Immunoblotting Analysis**—Protein samples were run on a 10% SDS-PAGE and transferred onto a nitrocellulose filter (MDI, India) as described previously (7, 8). Signal intensity of the immunoblot was quantitated using NIH Image software (ImageJ; National Institutes of Health).

## RESULTS

The characterization of laforin-deficient mice was reported in one of our previous publications (15). The present investigation was carried out on the C57BL/6 isogenic line for the *Epm2a* gene knock-out, derived by back-crossing the F1 heterozygous mutants with C57BL/6 animals through 11 generations, and the animals were genotyped as described (15).

**Neurofibrillary Tangles Observed in Laforin-deficient Mice**—Our investigations on the neuropathological changes in the brain sections of the 10-month-old laforin-deficient mice have suggested the presence of neurofibrillary tangles (NFTs), as revealed by Bielschowsky's silver staining (Fig. 1, A–C). This was subsequently confirmed by immunohistochemical staining with antibodies E178 (26) and AT8 (27, 28) that specifically recognize Tau protein phosphorylated at Ser<sup>396</sup> or Ser<sup>202</sup> residues, respectively (Fig. 1, D–I). Numerous neurons that were positive for the dyes or the phospho-Tau antibodies were seen primarily in the hippocampus, thalamus, cerebral cortex, cerebellum, and brain stem of the laforin-deficient mice but not in the corresponding regions of the wild-type littermates (Fig. 1, A–I). Identical observations were made with antibodies CP13 and PHF1 as well (supplemental Fig. S1, A–D). The NFTs in laforin-deficient mice also stained intensely with ubiquitin antibody (supplemental Fig. S1, E–G). NFTs were not observed in the 2-, 4-, or 6-month-old knock-out mice analyzed.

In addition to brain, Tau protein is known to express in muscle tissues (29, 30). We have therefore checked for the presence of hyperphosphorylation of Tau protein in the muscle tissues of the 10-month-old laforin-deficient mice. Phospho-Tau-specific antibodies identified immunoreactive cytoplasmic inclusions in the muscle sections from the knock-out mice but not the wild-type littermates (Fig. 1, J–M). Such inclusions were not seen in the muscle sections of 4- and 6-month-old knock-out mice.

**Biochemical and Ultrastructural Characterization of Tau in Laforin-deficient Mice**—Consistent with the immunohistochemical observations, immunoblot analysis of Tau protein from the 10-month-old animals showed a significant increase in the phosphorylation levels at the Ser<sup>202</sup> and Ser<sup>396</sup> positions, both in muscle and brain tissues of the laforin-deficient mice, as compared with the wild-type littermates (Fig. 2, A and B, and supplemental Fig. S2A). This difference, however, was not obvious in the 4-month-old mice (Fig. 2A). The phosphorylation levels of Tau were nearly the same in wild-type and heterozygous animals of the 10-month age group (supplemental Fig. S2C). Because Tau is known to form insoluble aggregates upon hyperphosphorylation (31, 32), we further assessed the amount of Tau in the Sarkosyl-insoluble fractions derived from the brain and muscle tissues of the 10-month-old animals. A large amount of insoluble and phosphorylated forms of Tau was recovered from the brain and muscle tissue lysates of the laforin-deficient mice as compared with lysates of wild-type littermates (Fig. 2C). The Sarkosyl-insoluble material recovered

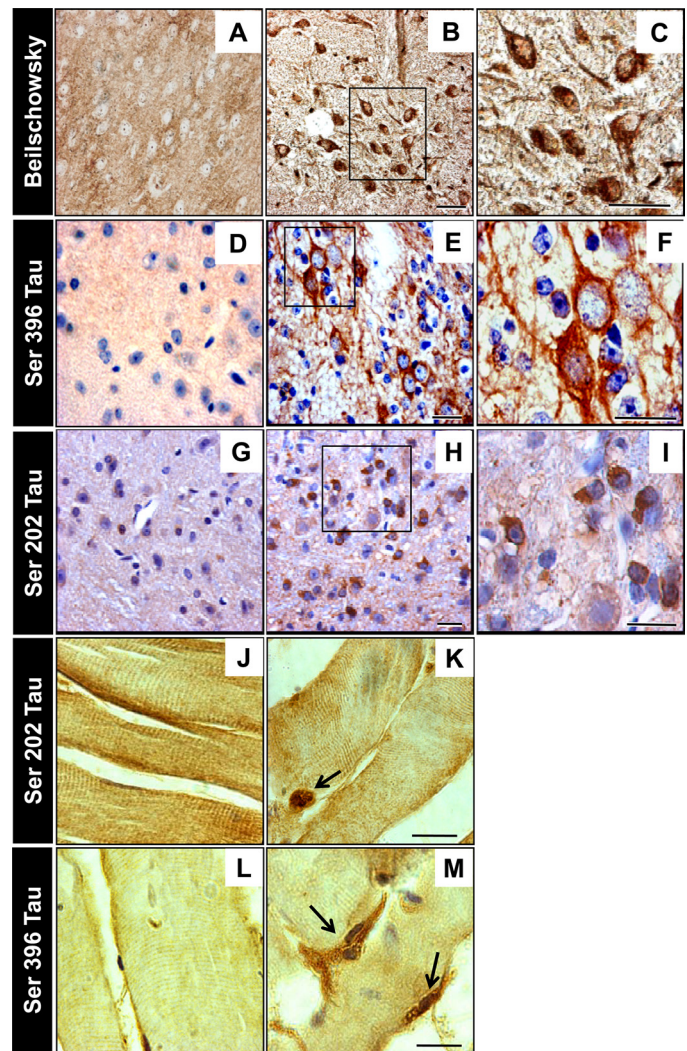


**FIGURE 1. Histochemical and immunohistochemical assessment of the brain and muscle sections from the wild-type and the *Epm2a* knock-out mice.** Shown is Bielschowsky's silver staining in the brain stem region of the 10-month-old wild-type (A) and the *Epm2a* knock-out mice brains (B and C), revealing neurofibrillary tangles. Shown are anti-Tau (E178 and AT8) immunoreactivity in the brain stem regions of the brain (D–I) or the skeletal muscle tissues (J–M) of the 10-month-old wild-type (D, G, J, and L) and the *Epm2a* knock-out mice, as indicated (E, F, H, I, K, and M). Scale bar, 30  $\mu$ m in A, B, D, E, G, and H; 10  $\mu$ m in C, F, and I; 20  $\mu$ m in J–M.

from the laforin-deficient mice was further investigated with transmission electron microscopy. The NFTs observed in the Sarkosyl-insoluble fraction appeared to be straight filaments of about 10–20 nm in diameter (Fig. 2D). Labeling with antibodies against phosphorylated Tau (Ser<sup>396</sup>) revealed reasonably abundant Tau-containing filaments in the preparation (Fig. 2, E and F). Such filaments were not seen in the preparations obtained from the age-matched wild-type littermates (data not shown), and the gold particles were not seen when the primary antibody was omitted for the immunodetection for the samples from the knock-out mice (data not shown). Taken together, the biochemical and ultrastructural analyses strongly suggest the presence of NFT-like Tau aggregates in the brain and muscle tissue of the laforin-deficient mice.

**Changes in the Phosphorylation Status of Tau Kinases and Tau Phosphatases in Laforin-deficient Mice**—Having established the difference in the phosphorylation levels of Tau pro-

## Hyperphosphorylation of Tau in Laforin-deficient Mice

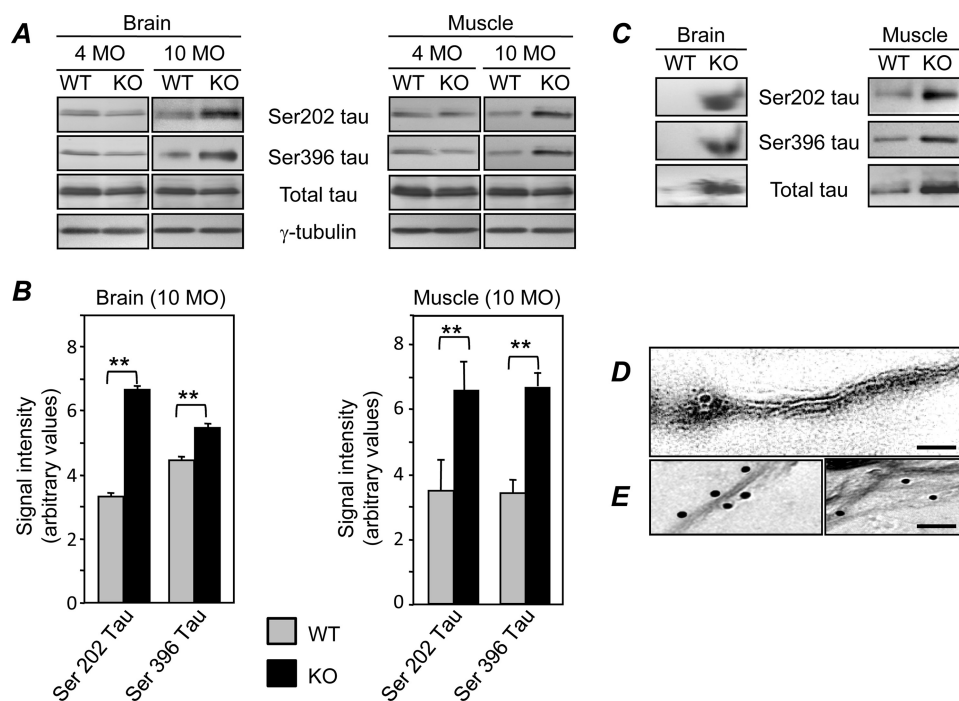


**FIGURE 2. Biochemical and electron microscopic analyses of Tau protein in laforin-deficient mice.** *A*, brain and muscle tissue lysates of 4- (4 MO) or 10-month-old (10 MO) *Epm2a* knock-out (KO) or the wild-type (WT) littermates were evaluated by using antibodies that detect changes in the phospho form (CP13 and PHF1) or the total form of Tau protein (TGF5) by immunoblotting, as indicated. *B*, bar diagram showing the difference in the signal intensity of different forms of Tau, as indicated. Each bar represents average values  $\pm$  S.D. of immunoblot analyses ( $n = 4$ ; \*\*,  $p < 0.005$ ). *C*, the detergent-insoluble Tau from brain and muscle tissues of 10-month-old animals were immunoblotted with (CP13, PHF1, and TGF5) antibodies raised against distinct forms of Tau, as indicated. *D*, electron microscopic analysis of Sarkosyl-insoluble NFTs isolated from the 10-month-old laforin-deficient mice as revealed by negative staining with 2% uranyl acetate. Most NFTs appeared to be straight filaments. *E*, purified NFTs were immunolabeled with an antibody against the Ser<sup>396</sup> phospho-Tau, followed by negative staining with phosphotungstic acid. The phospho-Tau antibody was detected with a 10-nm gold particle-conjugated secondary antibody. Scale bar, 50 nm.

tein in laforin-deficient mice, we next explored whether loss of laforin leads to changes in the phospho forms of key kinases and phosphatases that are known to regulate Tau. For this analysis, we have selected six kinases and two phosphatases (see Fig. 3). Activation of GSK3 $\beta$  is known to phosphorylate Tau protein (33, 34). The active and inactive forms of GSK3 $\beta$  were quantitated by looking at the phosphorylation status of Tyr<sup>216</sup> and Ser<sup>9</sup> residues by using antibodies that are specific to these two phospho forms (35, 36) and also by enzymatic assays using a substrate (Fig. 3, *A* and *B*). Although the total level of GSK3 $\beta$  was comparable among the wild-type and laforin-deficient animals, the levels of the inactive form of GSK3 $\beta$  (phospho-Ser<sup>9</sup>) were found to be significantly lower in the muscle and brain tissues of the 10-month-old knock-out mice (Fig. 3, *A* and *D*, and supplemental Fig. S2*B*). We therefore measured the GSK3 $\beta$  activity by <sup>32</sup>P labeling in an *in vitro* assay and found that the GSK3 $\beta$  from laforin-deficient mice indeed show increased activity as compared with that from age-matched wild-type mice (Fig. 3*B*). No difference in the phosphorylation levels of Tyr<sup>216</sup> residue was observed in the analyzed tissues of the two age groups (Fig. 3*A*).

Using a similar approach, we next examined how a few other regulators (kinases/phosphatases) might contribute to hyperphosphorylation of Tau protein in laforin-deficient mice. As shown in Fig. 3*C*, levels of CDK5 and its active form (CDK5-P), PKA and its active form (PKA-P), protein kinase B (AKT) and

its active form (AKT-P), PP2A and its active form (PP2A-P), and the total levels of PP1 were found to be similar among the wild-type and the knock-out mice littermates of the 10-month age group. Taken together, these results suggest that the contributions of these enzymes to Tau phosphorylation were not affected by the loss of laforin.

**Laforin Physically Interacts with and Dephosphorylates the Tau Protein**—Since the loss of laforin led to the hyperphosphorylation of Tau, we next explored the possibility that laforin, being a protein phosphatase, directly interacts with and dephosphorylates Tau. For this, polyhistidine-tagged Tau was transiently coexpressed with green fluorescent protein (GFP)-tagged laforin or GFP in COS-7 cells, and lysates were analyzed by nickel affinity bead pull-down assays. As can be seen in Fig. 4, Tau was able to pull down GFP-laforin and not the GFP, thus establishing the specific and physical interaction between laforin and Tau proteins. We next determined the domain of laforin that interacted with Tau. For this, we

created constructs that code for either the CBD or the DSPD of the laforin protein with the FLAG tag at the amino terminal (see Fig. 4*C*). His-tagged Tau was coexpressed with FLAG-tagged full-length laforin or its truncated forms (CBD or the DSPD) in COS-7 cells and processed for nickel affinity pull-down assays. As shown in Fig. 4*B*, Tau was able to pull the full-length laforin and the DSPD of laforin, but the truncated peptide having the CBD was not detected in the pulled-down products, suggesting that laforin interacts with Tau through its phosphatase domain. We have also checked the interaction between endogenous Tau and laforin using a coimmunoprecipitation approach. For this, we have used the brain tissue lysates from 10-month-old animals, pulled laforin using anti-laforin antibody, and checked for the presence of Tau protein in the pull-down products. As shown in Fig. 4*D*, Tau was detected in the pulled-down product from the wild-type tissue and not in the tissues from the laforin-deficient mice, confirming the interaction between laforin and Tau proteins and the specificity of the assay employed.

Having confirmed a direct physical interaction between laforin and Tau proteins, we next examined whether phosphorylated Tau is a substrate for laforin. For this, the wild-type Tau was expressed either alone or with laforin or an empty vector (control) in COS-7 cells and treated with wortmannin, a known inducer for Tau hyperphosphorylation (37). Similarly, a Tau missense mutant (P301L), which is

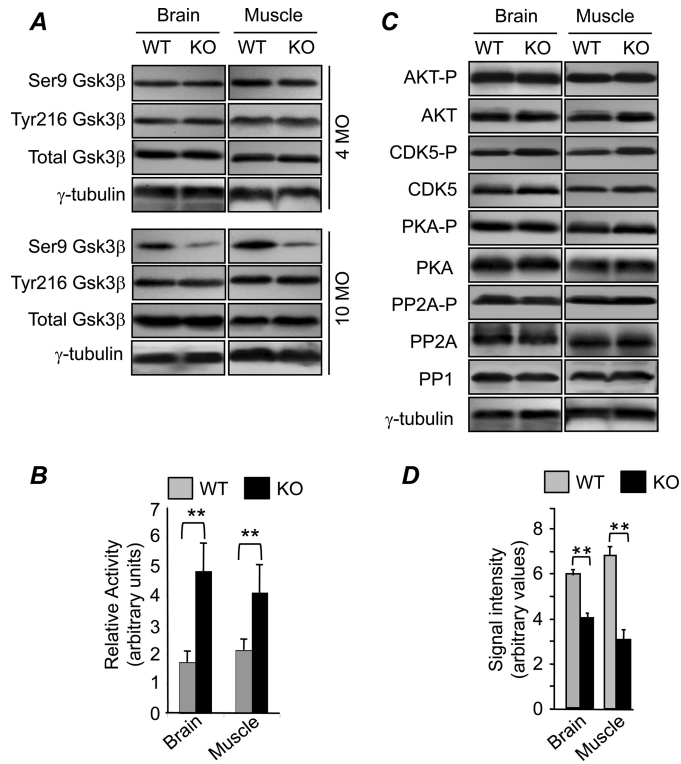


**FIGURE 3. Changes in kinases and phosphatases that regulate Tau phosphorylation.** *A*, lysates of brain and muscle tissues of 4- (4 MO) or 10-month-old (10 MO) *Epm2a* knock-out (KO) or wild-type (WT) littermates were analyzed with immunoblotting and antibodies against Ser<sup>9</sup> phospho-, Tyr<sup>216</sup> phospho-, or total form of GSK3 $\beta$ , as indicated. *B*, GSK3 $\beta$  activity assay was done on the brain and muscle tissue of the 10-month-old *Epm2a* knock-out (KO) or wild-type (WT) littermates. The bar diagram shows the difference in the relative activity of GSK3 $\beta$ , as indicated. Each bar represents average values  $\pm$  S.D. ( $n = 4$ ; \*\*,  $p < 0.005$ ). *C*, similarly, lysates from the brain and muscle tissues of the 10-month-old animals were tested for the following Tau kinases and phosphatases: Ser<sup>473</sup> phospho-AKT (AKT-P), total AKT, Ser<sup>159</sup> phospho-CDK5 (CDK5-P), total CDK5, Ser<sup>96</sup> phospho-PKA (PKA-P), total PKA, Tyr<sup>307</sup> phospho-PP2A (PP2A-P), total PP2A, and total PP1 antibodies. *D*, bar diagram showing the difference in the signal intensity of bands detected by antibody specific to phospho-GSK3 $\beta$  in the brain and muscle tissues in the 10-month-old animals. Each bar represents average values  $\pm$  S.D. ( $n = 4$ ; \*\*,  $p < 0.005$ ).

known to become hyperphosphorylated when overexpressed (31), was expressed either alone or with laforin. As shown in Fig. 5A, coexpression of laforin resulted in a significant reduction in the cellular levels of Ser<sup>396</sup> phospho form of both wild-type and the mutant Tau. Similarly, knockdown of laforin in a differentiated neuroblastoma cell line (Neuro2A) led to increased phosphorylation at the Ser<sup>396</sup> residue of endogenous Tau (Fig. 5B). To finally confirm that Tau is indeed a direct substrate of laforin, hyperphosphorylated Tau was purified and incubated with wild type or the mutant form of laforin, and the phosphorylation status at Ser<sup>396</sup> residue of Tau was evaluated by immunoblotting. Incubation of wild-type laforin with hyperphosphorylated Tau showed a significant reduction in the phosphorylation level at the Ser<sup>396</sup> residue as compared with reactions with the mutant laforin or the mock control (Fig. 5, C and D). These *in vitro* studies, in addition to replicating the findings in the laforin-deficient mice, have established that laforin indeed dephosphorylates the Ser<sup>396</sup> residue of Tau, and thus it is a Tau phosphatase. Knockdown of laforin or its overexpression did not alter the phosphorylation status of GSK3 $\beta$  at the Ser<sup>9</sup>

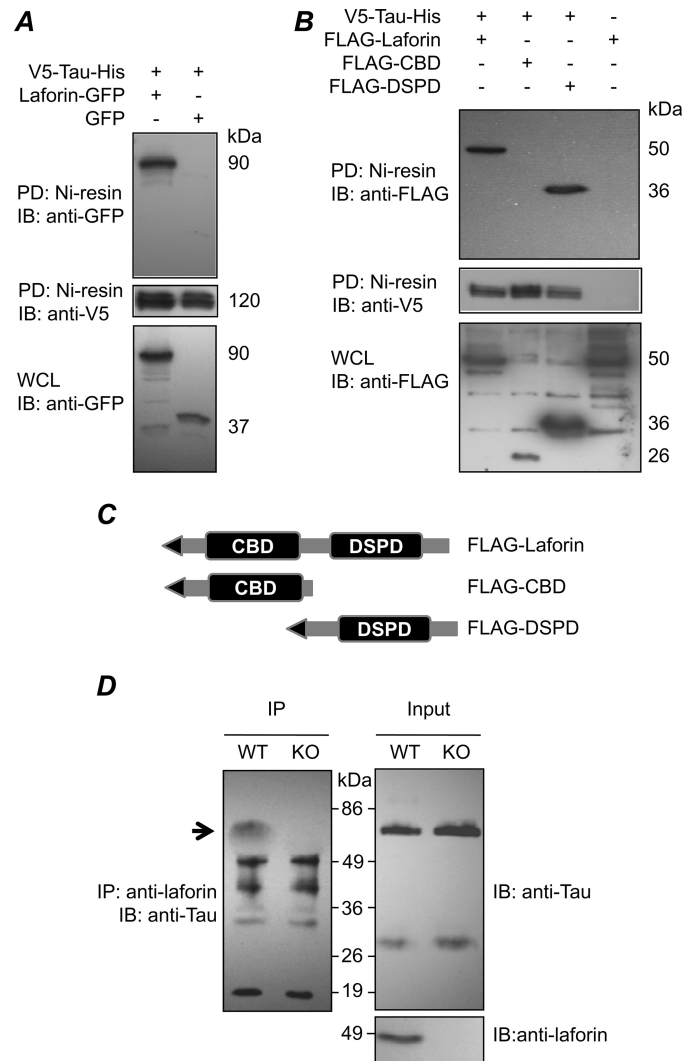


**FIGURE 4. Laforin physically interacts with Tau protein.** *A*, V5/His-tagged Tau was coexpressed with GFP-laforin or with GFP in COS-7 cells and processed for the pull-down assay using the nickel affinity resin. The pulled down products (PD) and whole cell lysates (WCL) were immunoblotted (IB) and probed with anti-GFP antibody and anti-V5 antibody. *B*, the phosphatase domain of laforin interacts with Tau protein. V5/His-tagged Tau protein was coexpressed in COS-7 cells with FLAG-tagged laforin, the CBD of laforin, or the DSPD and processed for the pull-down assay using the nickel affinity resin. The pulled down products and whole cell lysates were immunoblotted and probed with anti-FLAG and anti-V5 antibodies, as indicated. COS-7 cells that expressed FLAG-laforin only were processed for pull-down assay as control. As expected, anti-FLAG antibody did not detect any peptide in the pull-down product of this assay (last lane). *C*, schematic showing the domain organization of laforin protein and its truncated forms used for the pull-down assays. The amino-terminal triangles represent the FLAG epitope. *D*, co-immunoprecipitation analysis demonstrating the interaction between endogenous laforin and Tau proteins. Tissue lysates from 10-month old brain of wild-type (WT) or *Epm2a* knock-out mice (KO) were processed for immunoprecipitation with a rabbit polyclonal anti-laforin antibody, and the immunoprecipitated products (IP) were immunoblotted (IB) with an anti-Tau antibody raised in mice. Whole tissue lysates (input) were used as control. Note the presence of an  $\sim 66$  kDa Tau band (identified with an arrow) in the immunoprecipitated products in the tissue lysate from the wild-type but not from the knock-out mice.

position in the Neuro2A cell line (supplemental Fig. S2, D–E), suggesting that the observed difference in the phosphorylation status of GSK3 $\beta$  in the laforin-deficient mice could be a secondary effect and could be due to the physiological changes associated with loss of laforin in mice.

## Hyperphosphorylation of Tau in Laforin-deficient Mice

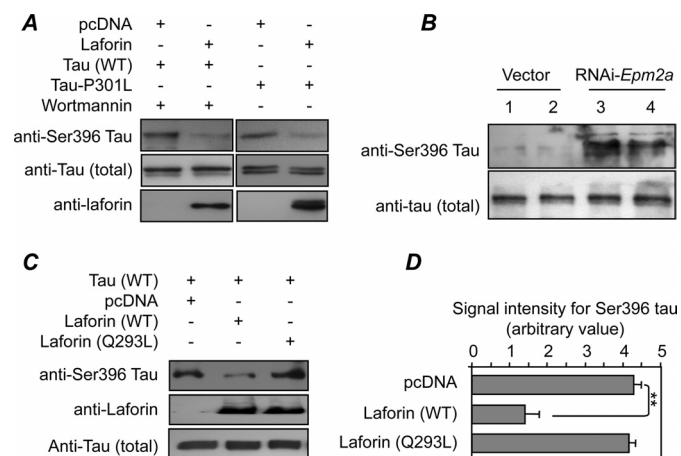


**FIGURE 5. Laforin dephosphorylates Tau protein at Ser<sup>396</sup> residue.** *A*, wild-type Tau or its mutant (P301L) was coexpressed with a construct for laforin or an empty vector in COS-7 cells and analyzed for the difference by immunoblotting with PHF1 antibody, as indicated. COS-7 cells expressing wild-type Tau were treated with wortmannin to induce hyperphosphorylation of Tau. *B*, Neuro2A cells were transfected with empty vector (vector; lanes 1 and 2), or the short hairpin RNA interference construct to silence the *Epm2a* gene (*RNAi-Epm2a*; lanes 3 and 4), differentiated into neurons, and analyzed for changes in the phospho form of endogenous Tau by immunoblotting with PHF1. The efficiency of *Epm2a* knockdown was previously established by immunoblotting with anti-laforin antibody (8). *C*, Tau, laforin, and laforin mutant were overexpressed in COS-7 cells, affinity-purified, and used for the *in vitro* dephosphorylation assay as indicated. Resins incubated with empty vector transfected (*pcDNA*) cells were used as control. The reaction was arrested and immunoblotted with antibodies as indicated, as discussed under "Experimental Procedures." *D*, bar diagram showing the difference in the signal intensity of bands detected by PHF1 antibody in the *in vitro* dephosphorylation assays done with the wild-type laforin, its mutant (Q293L), or the control resin (*pcDNA*). Each bar represents average values  $\pm$  S.D. ( $n = 3$ ; \*\*,  $p < 0.005$ ).

## DISCUSSION

In this report, we demonstrate that the loss of laforin leads to accumulation of hyperphosphorylated Tau as NFTs in the LD mice model. The observed NFTs were ubiquitinated and detergent-insoluble, as known in Alzheimer disease (18, 38, 39), and such forms were abundant in the 10-month-old knock-out mice, suggesting a progressive deterioration of brain function. The regions that were positive for the NFTs strongly correlated with the sites of laforin expression (40). NFTs were not seen in the heterozygote littermates, suggesting that the complete loss of laforin is required for its formation in LD. Curiously, Lafora bodies and neuronal cell death, the other two neuropathological changes observed in the knock-out mice, predate the NFT formation (15–17). Thus, the progressive onset of the LD-like symptoms observed in laforin-deficient mice seems to correlate well with the age-dependent deposition of NFTs in the brain (15). NFTs have also been reported in LD patients (41); thus, abnormal regulation of Tau protein appears to be one of the common neuropathological changes associated with LD in humans and mice. Intriguingly, Tau straight filaments have also been described in Alzheimer and Pick diseases (42, 43). Thus, the NFTs are likely to underlie a subset of symptoms of LD, like dementia, which is known in tauopathies as well (2).

One of the significant findings of the present study was the observation of NFTs in the muscle tissues of the laforin-deficient mice. NFTs in the skeletal muscle are known in several forms of myopathies that are characterized by progressive muscle weakness and atrophy (44, 45). Although muscular atrophy

is known in human LD (2), inclusions other than Lafora bodies in muscle have not yet been reported. Pending such findings, our present set of observations, together with our earlier report on muscular weakness in this LD mouse model (15), suggest that the Tau-positive inclusions could underlie some of the deficits of muscle functions seen in LD.

In determining which kinase or phosphatase is involved in the hyperphosphorylation of Tau in laforin-deficient mice, we show here that the level of the Ser<sup>9</sup>-phospho (inactive) form of GSK3 $\beta$  was lower in the 10-month-old knock-out mice. However, no changes in the level of the protein or in the phosphorylation levels were observed for several other players that are known to regulate the phosphorylation of Tau protein. Thus, the overactive GSK3 $\beta$  could be one of the triggers for the formation of NFTs in LD mice. Our observations on the GSK3 $\beta$  phosphorylation in the laforin-deficient mice and in cellular models contradict the report of Wang *et al.* (46) that the Ser<sup>9</sup> residue of GSK3 $\beta$  was dephosphorylated by laforin phosphatase and support an earlier report that GSK3 $\beta$  is not a substrate of laforin (11). Since there is a reduction in the phospho form of GSK3 $\beta$  in the knock-out mice, laforin probably acts upstream of this key enzyme. AKT, PKA, and PP1 are a few of the known regulators of the Ser<sup>9</sup> residue of GSK3 $\beta$  (36, 48, 49), and all three of them did not show a significant change in the phosphorylation level in the laforin-deficient mice. It would therefore be of interest to look for other regulators of GSK3 $\beta$  in the laforin-deficient mice.

Because laforin is a dual specificity phosphatase (4), we have also tested the possibility whether Tau could be a substrate for laforin. We demonstrate here that laforin physically interacts with Tau and that the interaction could perhaps be limited to the phosphatase domain of laforin. Consistent with the findings in the laforin-deficient mice, we show here with cellular models that coexpression of laforin with Tau decreases the phospho-Tau levels and that knockdown of laforin leads to an increase in the phospho form of Tau. Direct evidence for laforin being a Tau phosphatase came from the *in vitro* dephosphorylation assay. Thus, laforin might dephosphorylate Tau, at least at the Ser<sup>396</sup> residue, under appropriate physiological signals. Mutations resulting in the loss of laforin, its phosphatase activity, or its interaction with Tau would lead to hyperphosphorylation of Tau and the NFTs, as seen in the LD mice. It would be of much interest now to check the level and/or activity of laforin in tauopathies like Alzheimer disease.

Tau phosphorylation reflects a critical balance between Tau kinase and Tau phosphatase activities. We show here that loss of laforin is associated with an increase in the levels of active form of GSK3 $\beta$  in the LD model. Thus, NFTs in LD may both involve activation of the Tau kinase (GSK3 $\beta$ ) and the inactivation of a Tau phosphatase (laforin). GSK3 $\beta$  is known to act on Tau either individually or as a complex in the Alzheimer disease condition (35, 50). The activation of GSK3 $\beta$  in LD draws striking parallels with Alzheimer disease. Another element for Tau pathology in LD could be the Lafora polyglucosan bodies. Alterations in the glucose metabolism are associated with abnormal Tau phosphorylation (47, 51). Lafora bodies are thought to result from abnormal glycogen metabolic pathways (1, 11, 15, 16); therefore, a role for these inclusions in the genesis of NFTs cannot be ruled out.

In summary, we demonstrate here that loss of laforin leads to Tau hyperphosphorylation and NFTs, that laforin could be a crit-

ical regulator of Tau phosphorylation, and that the abnormal hyperphosphorylation of Tau might underlie some of the symptoms in LD. This study thus provides novel insight into the molecular basis of LD and has important implications on the formation of NFTs in tauopathies.

*Acknowledgments*—We thank Dr. Peter Davies (Albert Einstein College of Medicine) for the anti-Tau antibodies and Dr. Michael Hutton (Mayo Clinic College of Medicine) for the Tau expression constructs. We also thank Dr. Takumi Akagi (RIKEN Brain Science Institute, Wako-shi) and Dr. Gouthama (IIT Kanpur) for help and advice with the electron microscopy.

## REFERENCES

- Ganesh, S., Puri, R., Singh, S., Mittal, S., and Dubey, D. (2006) *J. Hum. Genet.* **51**, 1–8
- Van Heycop, D. E., and Jager, H. (1963) *Epilepsia* **4**, 95–119
- Minassian, B. A., Lee, J. R., Herbrick, J. A., Huizenga, J., Soder, S., Mungall, A. J., Dunham, I., Gardner, R., Fong, C. Y., Carpenter, S., Jardim, L., Satishchandra, P., Andermann, E., Snead, O. C., 3rd, Lopes-Cendes, I., Tsui, L. C., Delgado-Escueta, A. V., Rouleau, G. A., and Scherer, S. W. (1998) *Nat. Genet.* **20**, 171–174
- Ganesh, S., Agarwala, K. L., Ueda, K., Akagi, T., Shoda, K., Usui, T., Hashikawa, T., Osada, H., Delgado-Escueta, A. V., and Yamakawa, K. (2000) *Hum. Mol. Genet.* **9**, 2251–2261
- Chan, E. M., Young, E. J., Ianzano, L., Munteanu, I., Zhao, X., Christopoulos, C. C., Avanzini, G., Elia, M., Ackerley, C. A., Jovic, N. J., Bohlega, S., Andermann, E., Rouleau, G. A., Delgado-Escueta, A. V., Minassian, B. A., and Scherer, S. W. (2003) *Nat. Genet.* **35**, 125–127
- Gentry, M. S., Worby, C. A., and Dixon, J. E. (2005) *Proc. Natl. Acad. Sci. U.S.A.* **102**, 8501–8506
- Mittal, S., Dubey, D., Yamakawa, K., and Ganesh, S. (2007) *Hum. Mol. Genet.* **16**, 753–762
- Garyali, P., Siwach, P., Singh, P. K., Puri, R., Mittal, S., Sengupta, S., Parihar, R., and Ganesh, S. (2009) *Hum. Mol. Genet.* **18**, 688–700
- Ganesh, S., Tsurutani, N., Suzuki, T., Hoshii, Y., Ishihara, T., Delgado-Escueta, A. V., and Yamakawa, K. (2004) *Biochem. Biophys. Res. Commun.* **313**, 1101–1109
- Chan, E. M., Ackerley, C. A., Lohi, H., Ianzano, L., Cortez, M. A., Shannon, P., Scherer, S. W., and Minassian, B. A. (2004) *Hum. Mol. Genet.* **13**, 1117–1129
- Worby, C. A., Gentry, M. S., and Dixon, J. E. (2006) *J. Biol. Chem.* **281**, 30412–30418
- Vilchez, D., Ros, S., Cifuentes, D., Pujadas, L., Vallès, J., García-Fojeda, B., Criado-García, O., Fernández-Sánchez, E., Medraño-Fernández, I., Domínguez, J., García-Rocha, M., Soriano, E., Rodríguez de Córdoba, S., and Guinovart, J. J. (2007) *Nat. Neurosci.* **10**, 1407–1413
- Solaz-Fuster, M. C., Gimeno-Alcañiz, J. V., Ros, S., Fernandez-Sanchez, M. E., Garcia-Fojeda, B., Criado Garcia, O., Vilchez, D., Dominguez, J., Garcia-Rocha, M., Sanchez-Piris, M., Aguado, C., Knecht, E., Serratos, J., Guinovart, J. J., Sanz, P., and Rodriguez de Córdoba, S. (2008) *Hum. Mol. Genet.* **17**, 667–678
- Worby, C. A., Gentry, M. S., and Dixon, J. E. (2008) *J. Biol. Chem.* **283**, 4069–4076
- Ganesh, S., Delgado-Escueta, A. V., Sakamoto, T., Avila, M. R., Machado-Salas, J., Hoshii, Y., Akagi, T., Gomi, H., Suzuki, T., Amano, K., Agarwala, K. L., Hasegawa, Y., Bai, D. S., Ishihara, T., Hashikawa, T., Itohara, S., Cornford, E. M., Niki, H., and Yamakawa, K. (2002) *Hum. Mol. Genet.* **11**, 1251–1262
- Tagliabracci, V. S., Girard, J. M., Segvich, D., Meyer, C., Turnbull, J., Zhao, X., Minassian, B. A., Depaoli-Roach, A. A., and Roach, P. J. (2008) *J. Biol. Chem.* **283**, 33816–33825
- Machado-Salas, J., Guevara, P., Guevara, J., Martínez, I., Durón, R., Bai, D., Ganesh, S., Yamakawa, K., Suzuki, T., Amano, K., Cornford, E., and Delgado-Escueta, A. V. (2005) *Epilepsia* **46**, Suppl. 6, 75
- Sahara, N., Murayama, M., Mizorogi, T., Urushitani, M., Imai, Y., Takahashi, R., Murata, S., Tanaka, K., and Takashima, A. (2005) *J. Neurochem.* **94**, 1254–1263
- Yamamoto, T., and Hirano, A. (1986) *Neuropathol. Appl. Neurobiol.* **12**, 3–9
- Zhu, X., Raina, A. K., Rottkamp, C. A., Aliev, G., Perry, G., Boux, H., and Smith, M. A. (2001) *J. Neurochem.* **76**, 435–441
- Nangle, L. A., Zhang, W., Xie, W., Yang, X. L., and Schimmel, P. (2007) *Proc. Natl. Acad. Sci. U.S.A.* **104**, 11239–11244
- Petrucci, L., Dickson, D., Kehoe, K., Taylor, J., Snyder, H., Grover, A., De Lucia, M., McGowan, E., Lewis, J., Prihar, G., Kim, J., Dillmann, W. H., Browne, S. E., Hall, A., Voellmy, R., Tsuboi, Y., Dawson, T. M., Wolozin, B., Hardy, J., and Hutton, M. (2004) *Hum. Mol. Genet.* **13**, 703–714
- Dubey, D., and Ganesh, S. (2008) *Hum. Mol. Genet.* **17**, 3010–3020
- Ganesh, S., Tsurutani, N., Suzuki, T., Ueda, K., Agarwala, K. L., Osada, H., Delgado-Escueta, A. V., and Yamakawa, K. (2003) *Hum. Mol. Genet.* **12**, 2359–2368
- Loberg, R. D., Northcott, C. A., Watts, S. W., and Brosius, F. C., 3rd (2003) *Hypertension* **41**, 898–902
- Jakes, R., Novak, M., Davison, M., and Wischik, C. M. (1991) *EMBO J.* **10**, 2725–2729
- Biernat, J., Mandelkow, E. M., Schroter, C., Lichtenberg-Kraag, B., Steiner, B., Berling, B., Meyer, H., Mercken, M., Vandermeeren, A., Goedert, M., and Mandelkow, E. (1992) *EMBO J.* **11**, 1593–1597
- Goedert, M., Jakes, R., and Vanmechelen, E. (1995) *Neurosci. Lett.* **189**, 167–169
- Askanas, V., Engel, W. K., Bilak, M., Alvarez, R. B., and Selkoe, D. J. (1994) *Am. J. Pathol.* **144**, 177–187
- Mirabella, M., Alvarez, R. B., Bilak, M., Engel, W. K., and Askanas, V. (1996) *J. Neuropathol. Exp. Neurol.* **55**, 774–786
- Lewis, J., McGowan, E., Rockwood, J., Melrose, H., Nacharaju, P., Van Slegtenhorst, M., Gwinn-Hardy, K., Paul Murphy, M., Baker, M., Yu, X., Duff, K., Hardy, J., Corral, A., Lin, W. L., Yen, S. H., Dickson, D. W., Davies, P., and Hutton, M. (2000) *Nat. Genet.* **25**, 402–405
- Bandyopadhyay, B., Li, G., Yin, H., and Kuret, J. (2007) *J. Biol. Chem.* **282**, 16454–16464
- Sperber, B. R., Leight, S., Goedert, M., and Lee, V. M. (1995) *Neurosci. Lett.* **197**, 149–153
- Imahori, K., and Uchida, T. (1997) *J. Biochem.* **121**, 179–188
- Bhat, R. V., Shanley, J., Correll, M. P., Fieles, W. E., Keith, R. A., Scott, C. W., and Lee, C. M. (2000) *Proc. Natl. Acad. Sci. U.S.A.* **97**, 11074–11079
- Cross, D. A., Alessi, D. R., Cohen, P., Andjelkovich, M., and Hemmings, B. A. (1995) *Nature* **378**, 785–789
- Liu, S. J., Zhang, A. H., Li, H. L., Wang, Q., Deng, H. M., Netzer, W. J., Xu, H., and Wang, J. Z. (2003) *J. Neurochem.* **87**, 1333–1344
- Bancher, C., Grundke-Iqbal, I., Iqbal, K., Fried, V. A., Smith, H. T., and Wisniewski, H. M. (1991) *Brain Res.* **539**, 11–18
- Iqbal, K., and Grundke-Iqbal, I. (1991) *Mol. Neurobiol.* **5**, 399–410
- Ganesh, S., Agarwala, K. L., Amano, K., Suzuki, T., Delgado-Escueta, A. V., and Yamakawa, K. (2001) *Biochem. Biophys. Res. Commun.* **283**, 1046–1053
- Greene, V., and Pappasozomenos, S. C. (1987) *J. Neuropathol. Exp. Neurol.* **46**, 345
- Perry, G., Mulvihill, P., Manetto, V., Auttilio-Gambetti, L., and Gambetti, P. (1987) *J. Neurosci.* **7**, 3736–3738
- Kato, S., and Nakamura, H. (1990) *Acta Neuropathol.* **81**, 125–129
- Selcen, D., Ohno, K., and Engel, A. G. (2004) *Brain* **127**, 439–451
- Goebel, H. H., and Müller, H. D. (2006) *Semin. Pediatr. Neurol.* **13**, 96–103
- Wang, Y., Liu, Y., Wu, C., Zhang, H., Zheng, X., Zheng, Z., Geiger, T. L., Nuovo, G. J., Liu, Y., and Zheng, P. (2006) *Cancer Cell* **10**, 179–190
- Planel, E., Tatebayashi, Y., Miyasaka, T., Liu, L., Wang, L., Herman, M., Yu, W. H., Luchsinger, J. A., Wadzinski, B., Duff, K. E., and Takashima, A. (2007) *J. Neurosci.* **27**, 13635–13648
- Fang, X., Yu, S. X., Lu, Y., Bast, R. C., Jr., Woodgett, J. R., and Mills, G. B. (2000) *Proc. Natl. Acad. Sci. U.S.A.* **97**, 11960–11965
- Szatmari, E., Habas, A., Yang, P., Zheng, J. J., Hagg, T., and Hetman, M. (2005) *J. Biol. Chem.* **280**, 37526–37535
- Sato, S., Tatebayashi, Y., Akagi, T., Chui, D. H., Murayama, M., Miyasaka, T., Planel, E., Tanemura, K., Sun, X., Hashikawa, T., Yoshioka, K., Ishiguro, K., and Takashima, A. (2002) *J. Biol. Chem.* **277**, 42060–42065
- Planel, E., Miyasaka, T., Launey, T., Chui, D. H., Tanemura, K., Sato, S., Murayama, O., Ishiguro, K., Tatebayashi, Y., and Takashima, A. (2004) *J. Neurosci.* **24**, 2401–2411

## Supplemental Data:

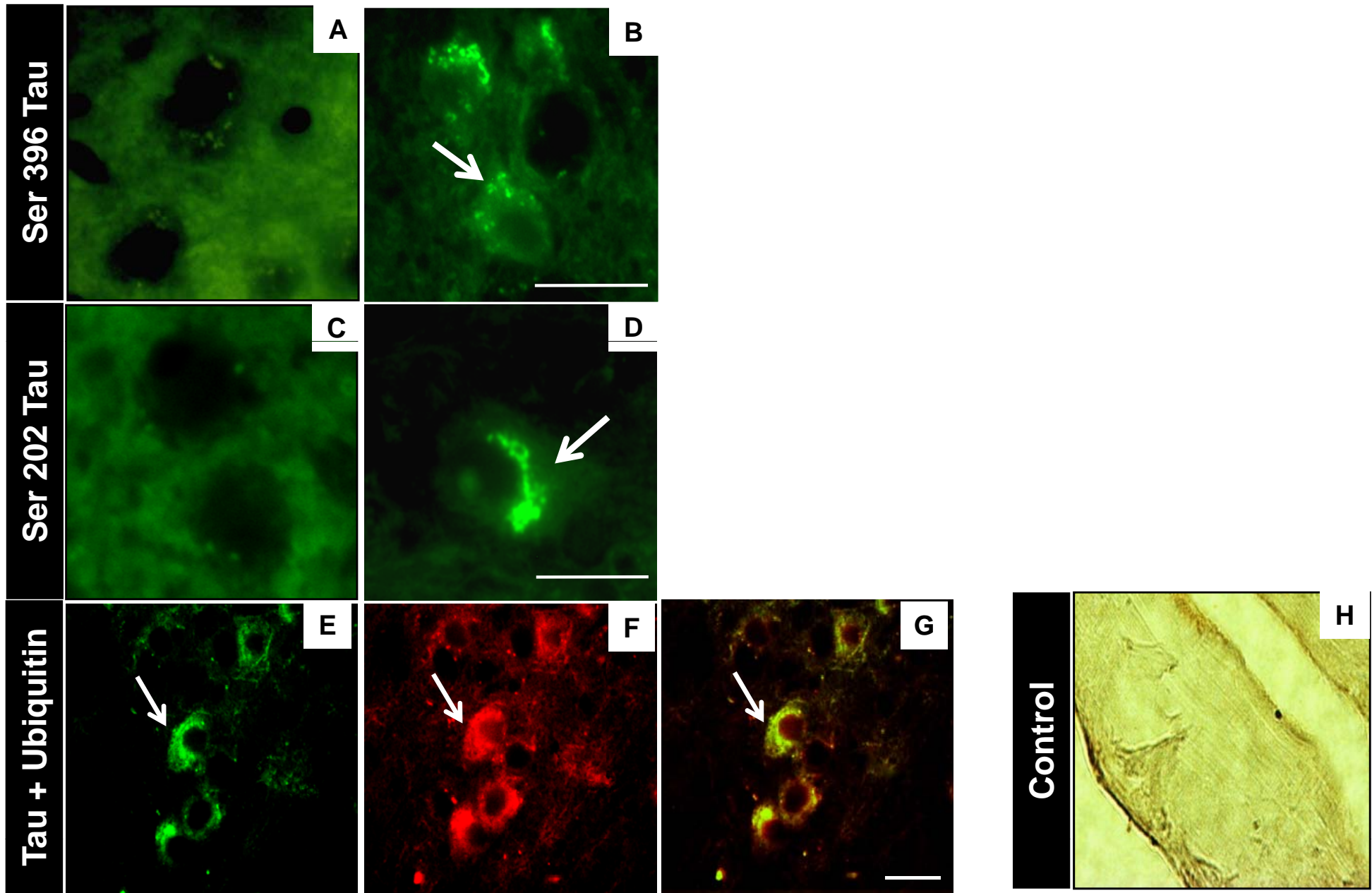
### Legend to supplemental figures (Fig. S1 and S2)

**Figure S1:** Tau protein immunoreactivity in the brain and muscle sections from wild-type (WT) and the *Epm2a* knockout (KO) mice. **A-D** Immunoreactive tau species, specific to phosphorylation dependent antibodies PHF1 and CP13 raised in mouse against the Ser396 or Ser202 phospho-tau, in the brains sections of *Epm2a* knockout (**B, D**) and not in the wild-type animals (**A, C**). Double immunofluorescence staining for PHF1 and ubiquitin in the 10 MO *Epm2a* knockout mice brain sections (**E, G**). The green (**E**) and red (**F**) signals identify tau and ubiquitin, respectively, and the yellow signals (**G**) reveal their co localization (merged image). Image **H** represent a control reaction for the knockout mice muscle section, where in the primary antibody was omitted. Scale bar: 10  $\mu\text{m}$  in **A, B, C** and **D**; 30  $\mu\text{m}$  in **E, F** and **G**; 20  $\mu\text{m}$  in **H**.

**Figure S2:** (A) Brain and muscle tissue lysates of 10-month-old (10 MO) *Epm2a* knockout (KO) or the wild-type (WT) littermates were evaluated by using antibodies that detect changes in the phospho- (CP13 and PHF1), or the total form of tau protein (TGF5) by immunoblotting, as indicated. (B) Lysates of brain and muscle tissues of 10-month-old *Epm2a* knockout (KO) or wild-type (WT) littermates were analyzed with immunoblotting and antibodies against Ser9 phospho-, Tyr216 phospho- or total form of GSK3 $\beta$ , as indicated. (C) Muscle tissue lysates of 10-month-old (10 MO) of wild-type (WT) and heterozygous (HT) littermates for the *Epm2a* knockout allele were evaluated by using antibodies that detect changes in the phospho forms of tau protein (antibody CP13 and PHF1) by immunoblotting, as indicated. (D) Neuro2A cells were transfected with either the empty vector or with a shRNA construct for the RNAi-mediated knockdown of the *Epm2a* transcripts, and the cell lysates immunoblotted for the detection of phospho or total form of GSK3 $\beta$  and laforin as indicated. (E) Neuro2A cells were transiently

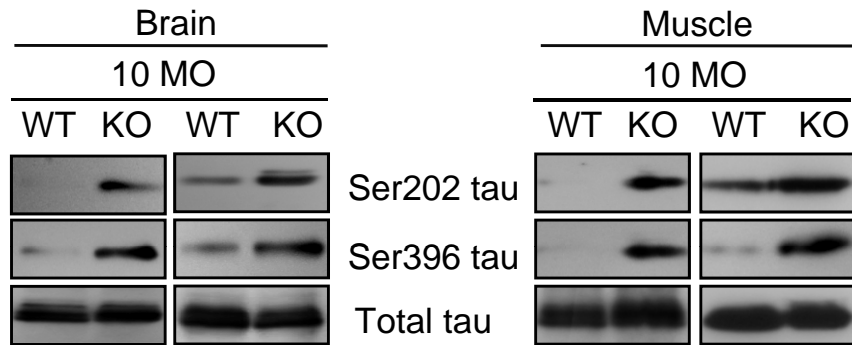
transfected with empty vector (pcDNA), vector expressing wild-type laforin (WT) or its dominant negative mutant (C266S), and the lysate were probed with antibodies that detect the Ser9 phospho form, all forms GSK3 $\beta$  or the Myc epitope as indicated.

Supplementary figure S1:

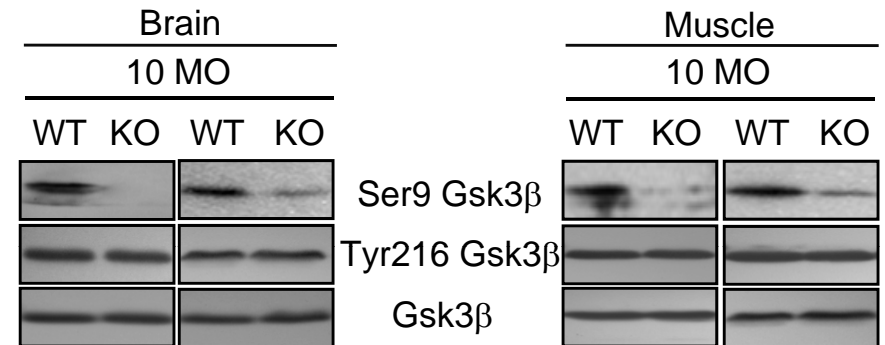


# Supplementary figure S2

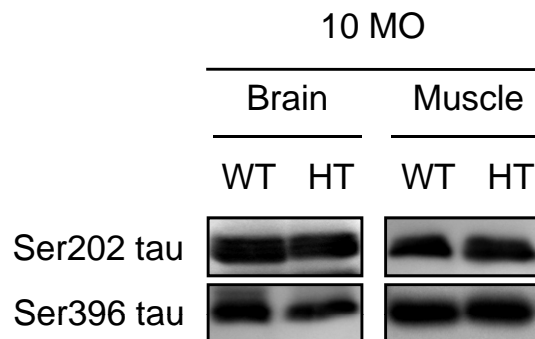
**A**



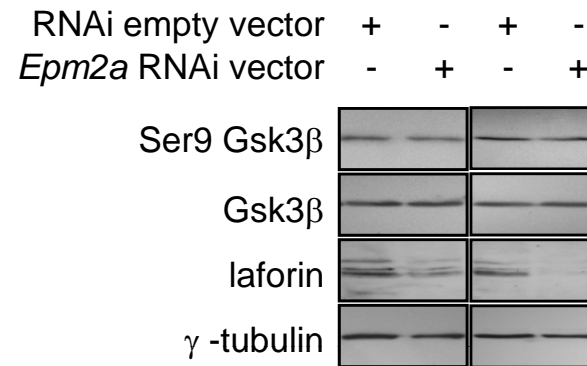
**B**



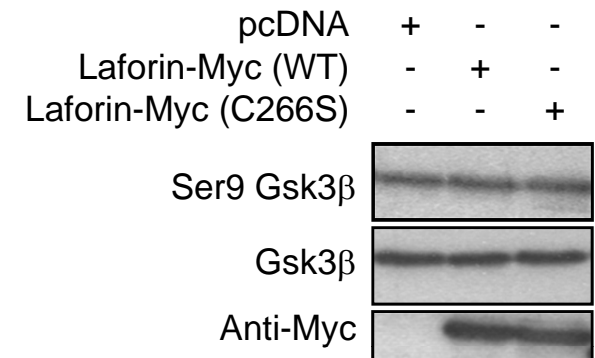
**C**



**D**



**E**



## **Hyperphosphorylation and Aggregation of Tau in Laforin-deficient Mice, an Animal Model for Lafora Disease**

Rajat Puri, Toshimitsu Suzuki, Kazuhiro Yamakawa and Subramaniam Ganesh

*J. Biol. Chem.* 2009, 284:22657-22663.

doi: 10.1074/jbc.M109.009688 originally published online June 19, 2009

---

Access the most updated version of this article at doi: [10.1074/jbc.M109.009688](https://doi.org/10.1074/jbc.M109.009688)

### Alerts:

- [When this article is cited](#)
- [When a correction for this article is posted](#)

[Click here](#) to choose from all of JBC's e-mail alerts

### Supplemental material:

<http://www.jbc.org/content/suppl/2009/06/18/M109.009688.DC1.html>

This article cites 51 references, 25 of which can be accessed free at <http://www.jbc.org/content/284/34/22657.full.html#ref-list-1>